2014 IEEE 14th International Conference on Bioinformatics and Bioengineering

Computer Simulation of Hot Caloric Test Response in the Three Semicircular Canal

Nenad Filipovic, *Member, IEEE*, Igor Saveljic and Zarko Milosevic

Abstract—**In this study we investigated the hot caloric test response in the three semicircular canals using coupled fluid flow, natural convection and fluid-structure interaction with the finite element method. We demonstrated that the temperature distribution of the horizontal canal duct is more dominant and a longer period of irrigation time is required in order to stimulate the two other vertical canals. Our results also show shear stress and force distribution from endolymph flow during natural convection. Future studies are necessary for validation of the presented computer model with clinical measurements.**

***Index Terms*— hot caloric test, computer model, shear stress, force, temperature distribution**

I. Introduction

The caloric test allows separate evaluation of one horizontal semicircular canal at a time by measuring the resulting nystagmus response in each eye representing each ear at low frequency. There are different the caloric test technique, as follows:

1) air or water stimulation caloric testing;
2) monothermal caloric testing;
3) ice water caloric testing;
4) directional preponderance and labyrinthic predominance: concepts, reference values and associated diseases;
5) areflexia, hyporeflexia and hypereflexia: concepts, reference values and associated diseases;
6) variables and artifacts that affect the caloric response: lighting, temperature, habituation, anxiety, status of the tympanic membrane, use of drugs, blinking of the eyes, Bell's phenomenon [1].

Caloric stimulation may be done with water or air; it generates an endolymphatic current within the stimulated lateral canal, analogous to a 0.003 Hz angular movement [2]. Knowing that the semicircular canals respond more efficiently to angular movements at 1 to 6Hz, it may be concluded that caloric testing assess the labyrinth in a non-physiological frequency [3].

This work was supported by FP7-ICT-2013-10 EMBalance project and Serbian Ministry of Education with Science Projects III-41007 and ON-174028.

N. Filipovic, I. Saveljic and Z. Milosevic are with BioIRC doo Kragujevac and the Faculty of Engineering, University of Kragujevac, Sestre Janjica 6, 34000 Kragujevac, Serbia (corresponding author phone: 381-34-334379; fax: 381-34-333192; e-mail: fica@kg.ac.rs;).

The caloric response is connected with the central nervous system, which is important in differentiating between central and peripheral vestibular diseases.

In the caloric test, the sensory organ on one side of the head is locally cooled (or warmed) by pouring cool (or warm) water into the external auditory meatus. By tilting the head back to the proper angle, a warm water stimulus will cause convection currents in the fluid filled vestibular end organ resulting in neural excitation of the central vestibular pathways.

Barany [4] described water caloric stimulation, and Fitzgerald and Hallpike [5] established its standard protocol. The ear is water-irrigated for 40 seconds at temperatures of 44°C and 30°C, 7°C over and 7°C below the bodily temperature, which generates the endolymphatic current [2].

Using warm water in the right ear, an ocular nystagmus is evoked in which the slow phase is towards the left side, and conversely the fast phase is towards the right. Cold water will have the opposite effect. The patterns of nystagmus evoked by this artificial stimulus provide important clinical clues regarding the integrity of both peripheral and central vestibular function.

The basic caloric test description has been presented in Fig. 1.

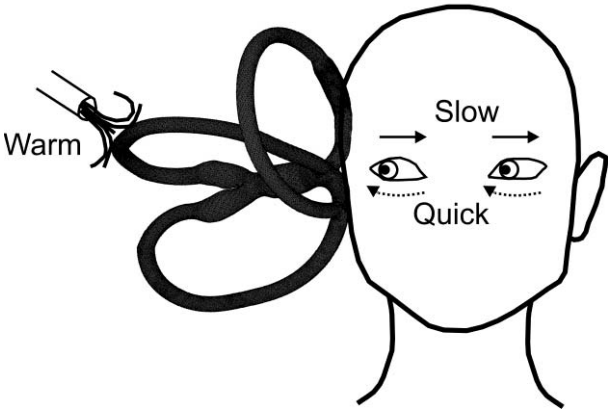

Fig. 1 Description of hot caloric test. Ocular nystagmus is evoked in which the slow phase is towards the left side, and conversely the fast phase is towards the right

Zucca et al. [6] and Valli et al. [7] investigated caloric response and they concluded that the gravity-dependent

978-1-4799-7502-0/14 $31.00 © 2014 IEEE
DOI 10.1109/BIBE.2014.48

buoyancy force is the largest contributor to the caloric response. Kassemi et al. [8] argued that the previous researchers did not incorporate the effects of fluid dynamics, and they further discovered through a finite element (FE) study that the dominant mechanism is the natural convection driven by the temperature-dependent variation in the bulk fluid. Still Barany's convection hypothesis remains largely acceptable to the majority of the vestibular community [5]. The caloric response in vertical canals still has an insufficient quantitative description. Shen et al. [9] give more insight in qualitative description of this phenomenon. We tried to extend this computer model to more human specific model.

The paper is organized as following. We firstly described numerical model with fluid flow, Navier-Stokes, continuity, thermodynamic and nonlinear solid mechanics equations. Basic parameters are described. In the section results we presented numerical simulations with shear stress, force, and temperature distribution during hot caloric test in time. Finally some conclusions are given.

II. METHODS

Mesh moving algorithm

The governing equations for simulation of endolymph flow include the Navier-Stokes equations of balance of linear momentum and the continuity equation with application of ALE formulation as [10].

$$\rho\left[v_i^{*} + \left(v_j - v_j^{m}\right)v_{i,j}\right] = -p_{,i} + \mu v_{i,jj} + f_i^{B} \qquad (1)$$

$$v_{i,i} = 0 \qquad (2)$$

where v_i and v_i^m are the velocity components of a fluid and of the point on the moving mesh occupied by the fluid particle, respectively; ρ is fluid density, p is fluid pressure, μ is dynamic viscosity, and f_i^B are the body force components (gravity). The symbol "*" denotes the mesh-referential time derivative, i.e. the time derivative at a considered point on the mesh,

$$(\ )^{*} = \left.\frac{\partial(\ )}{\partial t}\right|_{\xi_i = const} \qquad (3)$$

and the symbol "$_{,i}$" denotes partial derivative, i.e.

We use x_i and ξ_i as Cartesian coordinates of a generic particle in space and of the corresponding point on the mesh, respectively. The repeated index means summation, from 1 to 3, i.e. j=1,2,3 in Eq. (1), and i=1,2,3 in Eq. (2). In deriving Eq. (1) we used the following expression for the material derivative (corresponding to a fixed material point) $D(\rho v_i)/Dt$,

$$\frac{D(\rho v_i)}{Dt} = \left.\frac{\partial(\rho v_i)}{\partial t}\right|_{\xi} + (v_j - v_j^{m})\frac{\partial(\rho v_j)}{\partial x_i} \qquad (4)$$

The derivatives on the right-hand side correspond to a generic point on the mesh, with the mesh-referential derivative and the convective term.

Using the linearization (4) we obtain from (1) and (2) the system of ordinary differential equations in the form

$${}^{t}\mathbf{M}_{(1)}\mathbf{V}^{*} + {}^{t}\mathbf{K}_{(1)vv}\Delta\mathbf{V} + {}^{t}\mathbf{K}_{vp}\Delta\mathbf{P} = {}^{t+\Delta t}\mathbf{F}_{(1)} - {}^{t}\mathbf{F}_{(1)} \qquad (5)$$

and

$${}^{t}\mathbf{M}_{(2)}\mathbf{V}^{*} + {}^{t}\mathbf{K}_{(2)vv}\Delta\mathbf{V} = {}^{t+\Delta t}\mathbf{F}_{(2)} - {}^{t}\mathbf{F}_{(2)} \qquad (6)$$

The matrices and vectors follow from the volume and surface integrals given in [10].

Thermodynamics equations are:

$$\rho_0 c T^{*} + \rho_0 c\left(v_i - v_i^{m}\right)_{,i} T = kT_{,ii} \qquad (7)$$

$$\rho = \rho_0\left[1 - \beta_T\left(T - T_0\right)\right] \qquad (8)$$

where ρ_0 is initial density, β_T is thermal expansion coefficient, c is heat capacity and k is thermal conductivity of fluid.

Fluid-structure interaction

For fluid-structure interaction problem we use loose coupling methodology. The tissue of SSC has nonlinear constitutive laws, leading to materially-nonlinear finite element formulation. For a nonlinear wall tissue problem, the incremental-iterative equation is using:

$${}^{n+1}\hat{\mathbf{K}}_{tissue}^{(i-1)}\Delta\mathbf{U}^{(i)} = {}^{n+1}\hat{\mathbf{F}}^{(i-1)} - {}^{n+1}\mathbf{F}^{\mathrm{int}(i-1)} \qquad (9)$$

where $\Delta\mathbf{U}^{(i)}$ are the nodal displacement increments for the iteration '*i*', and the system matrix ${}^{n+1}\hat{\mathbf{K}}_{tissue}^{(i-1)}$, the force vector ${}^{n+1}\hat{\mathbf{F}}^{(i-1)}$ and the vector of internal forces ${}^{n+1}\mathbf{F}^{\mathrm{int}(i-1)}$ correspond to the previous iteration

The geometrically linear part of the stiffness matrix, $\left({}^{n+1}\mathbf{K}_{L}\right)_{tissue}^{(i-1)}$, and nodal force vector, ${}^{n+1}\mathbf{F}^{\mathrm{int}(i-1)}$, are defined:

$$\left({}^{n+1}\mathbf{K}_{L}\right)_{tissue}^{(i-1)} = \int_{V} \mathbf{B}_{L}^{T}\, {}^{n+1}\mathbf{C}_{tissue}^{(i-1)}\, \mathbf{B}_{L}\, dV,$$
$$\left({}^{n+1}\mathbf{F}^{\mathrm{int}}\right)^{(i-1)} = \int_{V} \mathbf{B}_{L}^{T}\, {}^{n+1}\boldsymbol{\sigma}^{(i-1)}\, dV \qquad (10)$$

where the consistent tangent constitutive matrix ${}^{n+1}\mathbf{C}_{tissue}^{(i-1)}$ of tissue and the stresses at the end of time step ${}^{n+1}\boldsymbol{\sigma}^{(i-1)}$ depend on the material model used. Calculation of the matrix ${}^{n+1}\mathbf{C}_{tissue}^{(i-1)}$ and the stresses ${}^{n+1}\boldsymbol{\sigma}^{(i-1)}$ for the tissue material models are performed at each iteration.

The overall strategy of fluid-structure interaction adopted here consists of the following steps [10]:

a) For the current geometry of the endolymph vessel, determine endolymph flow (with use of the ALE formulation when the wall displacements are large). Wall velocities at the common endolymph – endolymph surface are taken as the boundary condition for the fluid.
b) Calculate the loads, arising from the endolymph, which act on the walls.
c) Determine deformation of the walls taking the current loads from the endolymph.
d) Check for the overall convergence which includes fluid and solid. If convergence is reached, go to the next time step. Otherwise go to step a).

Update endolymph domain geometry and velocities at the common solid-fluid boundary for the new calculation of the endolymph flow. In case of large wall displacements, update the FE mesh for the endolymph flow domain. Go to step a).

Definition of coordinate system and finite element mesh of 3D human membranous labyrinth is presented in Fig. 2.

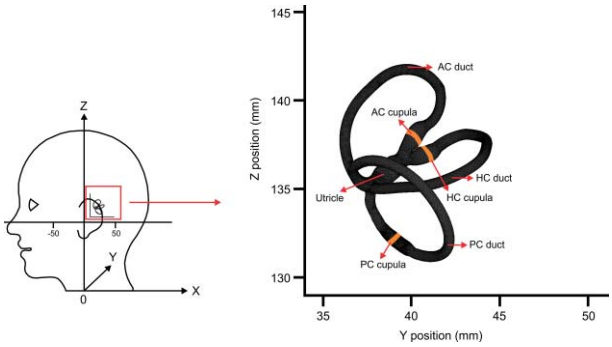

Fig. 2 Definition of coordinate system and finite element mesh of 3D human membranous labyrinth

The position of heated section is presented in Fig. 3

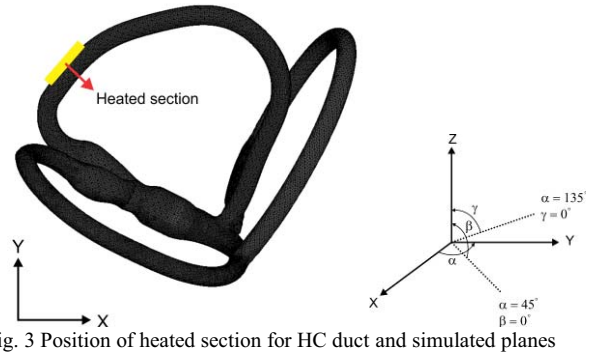

Fig. 3 Position of heated section for HC duct and simulated planes

The physical and structural properties of the endolymph and cupula are taken from literature [9].

III. RESULTS

We presented dynamics response of the SSC caloric test. The time is one second after hot contact where the temperature at the region near the hot contact rises rapidly. In this way temperature changes makes variation of the density of the endolymph. The natural convection moves the endolymph in HC duct. The velocity in the two vertical SSC is also generated. The flow induces the HC cupula deformation due to fluid forces which act on the cupula wall.

Shear stress distribution has been shown in Fig. 4. It can be seen that more dominant maximum shear stress distribution is presented on the cupula walls.

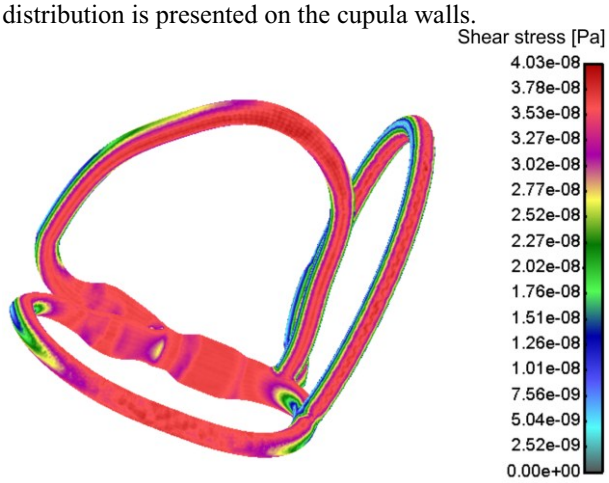

Fig 4. Shear stress distribution

The forces which act from endolymph flow and natural convection are presented in Fig. 5.

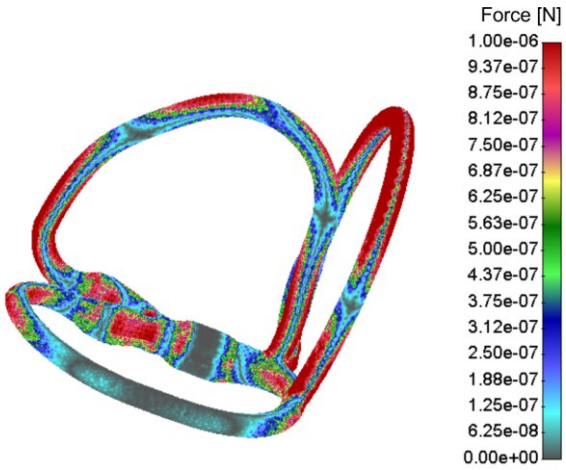

Fig 5. Distribution of the forces which act from endolymph side

It can be seen that HC cupula received smaller amount of the forces from fluid side than other parts of the SSC walls, but this HC cupula part is responsible for deflection and sensation of the cells for brain information.

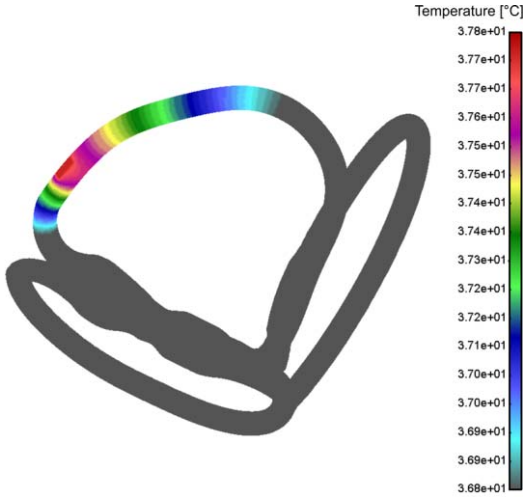

Fig. 6. Temperature distribution after 1 s

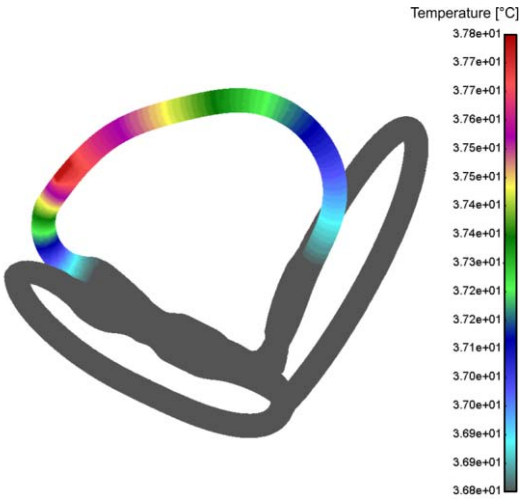

Fig. 7. Temperature distribution after 40 s

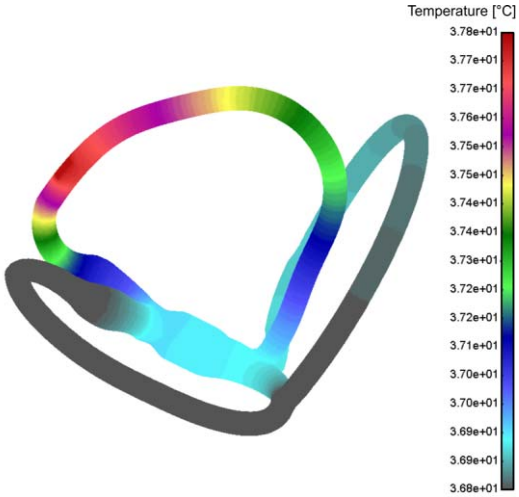

Fig. 8. Temperature distribution after 300 s

Temperature distribution in three SSC after 1s, 40s and 300s has been shown in Figs. 6-8 respectively. It can be seen that mostly temperature changes are dominant in HC duct.

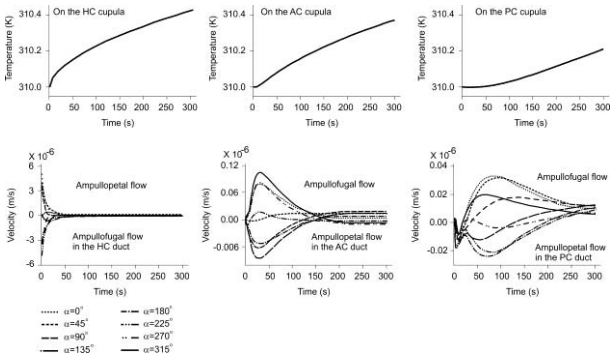

Fig. 9. Caloric response when the gravity force is parallel to the plane α. Temperature and endolymph velocity distribution in time.

Temperature and endolymph velocity distribution in time for the caloric response when the gravity force is parallel to the plane α (see Fig 3) has been presented in the Fig. 9.

IV. Conclusions

We presented in this study finite element model of hot caloric test response in 3D semicircular canals.
The temperature distribution results show that HC duct is more dominant and a longer period of irrigation time is required in order to stimulate the two other vertical canals. We also investigated shear stress and force distribution from endolymph flow during natural convection. Future research will go in the direction for validation of our model with human measurements for hot caloric test.

References

[1] DU Gonçalves, L Felipe, T Mara, A Lima, Interpretation and using of caloric testing, Rev Bras Otorrinolaringol;74(3):440-6. 2008.

[2] TP Zajonk, PS Roland, Vertigo and motion sickness. Part I: vestibular anatomy and physiology. Ear Nose Throat J 84(9):581-4. 2005.

[3] RD Tomlinson, GE Saunders, DWF Schwartz, Analysis of human vestibulo-ocular reflex during active head movements. Acta Otolaryngol ;90:184-90. 1980.

[4] R. Barany, Untersuchengen uber den vom vestibulapparat des ohres reflectorish ausgelosten rhytmischen nystagmus und seine begleiterscheinungen. Monatschr Ohrenheilk,40:193-297. 1906.

[5] G. Fitzgerald, CS Hallpike, Studies in human vestibular function I: observations on the directional preponderance of caloric nystagmus resulting from cerebral lesions. Brain 62:115-37. 1942.

[6] G. Zucca, L. Botta, S. Valli et al., Effects of caloric stimuli on frog ampullar receptors, Hearing Research, vol. 137, no. 1-2, pp. 8–14, 1999.

[7] P. Valli, A. Buizza, L. Botta, G. Zucca, L. Ghezzi, and S.Valli, Convection, buoyancy or endolymph expansion: what is the actual mechanism responsible for the caloric response of semicircular canals? Journal of Vestibular Research, vol. 12, no.4, pp. 155–165, 2003.

[8] M. Kassemi, J. G. Oas, and D. Deserranno, Fluid-structural dynamics of ground-based and microgravity caloric tests, Journal of Vestibular Research, vol. 15, no. 2, pp. 93–107, 2005.

[9] H. Scherer, U. Brandt, and A. H. Clarke, European vestibular experiments on the Spacelab-1 mission: 3. Caloric nystagmus in microgravity, Experimental Brain Research, vol. 64, no. 2, pp. 255–263, 1986.

[10] N. Filipovic, S. Mijailovic, A Tsuda, M Kojic, An implicit algorithm within the Arbitrary Lagrangian-Eulerian formulation for solving incompressible fluid flow with large boundary motions. Comp. Meth. Appl. Mech. Eng. 195:6347-6361, 2006.